Published in final edited form as:
Biotechnol Bioeng. 2010 January 1; 105(1): 121–129. doi:10.1002/bit.22525.

Aggregation of a Monoclonal Antibody Induced by Adsorption to Stainless Steel

Jared S. Bee[1], **Michele Davis**[1], **Erwin Freund**[2], **John F. Carpenter**[3], and **Theodore W. Randolph**[1]

[1]Department of Chemical and Biological Engineering, University of Colorado, Boulder, Colorado 80309

[2]Drug Product & Device Development, Amgen Inc., Thousand Oaks, CA 91320

[3]Department of Pharmaceutical Sciences, University of Colorado Health Sciences Center, Denver, Colorado 80262

Abstract

Stainless steel is a ubiquitous surface in therapeutic protein production equipment and is also present as the needle in some pre-filled syringe biopharmaceutical products. Stainless steel microparticles can cause of aggregation of a monoclonal antibody (mAb). The initial rate of mAb aggregation was second-order in steel surface area and zero-order in mAb concentration, generally consistent with a bimolecular surface aggregation being the rate-limiting step. Polysorbate 20 (PS20) suppressed the aggregation yet was unable to desorb the firmly bound first layer of protein that adsorbs to the stainless steel surface. Also, there was no exchange of mAb from the first adsorbed layer to the bulk phase, suggesting that the aggregation process actually occurs on subsequent adsorption layers. No oxidized Met residues were detected in the mass spectrum of a digest of a highly aggregated mAb, although there was five-fold increase in carbonyl groups due to protein oxidation.

Keywords

protein aggregation; kinetics; mechanism; adsorption; microparticles; injectors; stability; processing; biotechnology; monoclonal antibody; stainless steel; needle

INTRODUCTION

Protein aggregates contained in therapeutic protein formulations may sometimes cause adverse reactions in patients.[1,2] Formulation conditions are often chosen to maximize the thermodynamic and colloidal stability of the bulk protein to obtain a shelf life of about 2 years.[3] This strategy is based upon the classic Lumry-Eyring model of protein aggregation, where either unfolding or aggregate assembly can be the rate-determining aggregation step for bulk aggregation in solution.[3,4] Surfactants are also often added to protect against interfacial damage. The rate of protein aggregation in bulk solutions incubated under "accelerated" conditions (e.g., at elevated temperatures) are used to predict longer-term storage stability.[3,5] However, even after formulations are optimized for bulk stability, interactions of the protein with solid surfaces or particulate contamination may still cause aggregation. For some selected examples of surface-induced protein damage see.[6] Stainless steel, a ubiquitous surface in bioprocessing, has been shown to cause aggregation of

Correspondence to: Theodore W. Randolph (Telephone: 303-492-4776); Theodore.Randolph@colorado.edu; Fax: 303-492-4341).

monoclonal antibodies. Two different IgG4 mAbs were found to aggregate according to first order kinetics when exposed to stainless steel under high shear conditions.[7] In a different study, exposure of an IgG to stainless steel particulates, either shed from a filler pump or spiked into solution, caused the generation of much larger particles even when formulated with a non-ionic surfactant.[8] Fe ions leached from steel have been reported to cause oxidation of proteins resulting in aggregation. [9,10] Solution conditions may be critical: chloride ions increased the leaching of Fe ions from steel and it has been suggested the protein itself can cause corrosion of the steel surface.[9,10]

In our previous work we found that the same mAb used in the current study adsorbed to stainless steel particles with a loading of 1.06 mg/m^2 (in 10 mM sodium acetate buffer at pH 5.0).[6] Soluble aggregates were formed upon incubation of mAb with steel, yet aggregates were not formed by exposure of the mAb to the supernatant from the steel particles.[6] This strongly suggests that aggregation was caused by surface-mediated process such as surface-induced unfolding of the mAb, rather than by soluble species that dissolve from stainless steel surfaces. It is also possible that adsorption to stainless steel exposes buried residues, which are then oxidized, ultimately leading to aggregation. The rate-determining aggregation step might still be unfolding even if the microscopic step that ultimately causes aggregation could be the oxidation of a freshly exposed residue. Following this line of reasoning, adsorption-induced exposure of buried residues could potentially act in synergy with any chemical change (e.g. oxidation, hydrolysis, carbonylation, or deamidation), resulting in severe structural destabilization followed by aggregation.

Surface-induced protein aggregation could potentially occur by a variety of different mechanisms, resulting in different reaction orders in surface area and protein concentration.[11] By direct analogy with the Lumry-Eyring aggregation model, we expect that (partial) unfolding of the protein on the surface would be required in a surface-mediated aggregation mechanism. For physical aggregation processes, the rate-determining step could then be either the surface-induced unfolding or an assembly processes, such as: desorption/exchange of perturbed adsorbed proteins with bulk proteins, assembly of aggregates on the surface, or direct aggregation of bulk proteins onto unfolded nuclei on the surface. Chemical modification of structurally perturbed proteins could act in synergy with these physical processes. We note that actual bulk protein aggregation kinetics can be very complicated,[12] and even apparently simple reactions involving surfaces may also have complex rate behavior.[11] Potential synergies of different factors and the intricacies of protein biophysics add to the overall challenge of obtaining a fundamental understanding of these systems. Importantly, we believe that surface-induced protein aggregation will not necessarily have the same dependence on the thermodynamic or colloidal stability of the protein as is observed for bulk aggregation. This would explain why otherwise stable protein formulations may be subject to aggregation after exposure to specific surfaces and also hints that formulation conditions that minimize surface-induced aggregation may not necessarily always coincide with the optimal bulk solution formulation.

In this work we investigated the stainless steel-induced aggregation process using the initial rate method to determine the order of reaction with respect to steel surface area and protein concentration. To qualitatively differentiate between the different possible mechanisms discussed above we performed some additional measurements: fluorescent labeling was used to determine if adsorbed proteins can be displaced or exchanged with bulk proteins; dynamic light scattering was used as a sensitive probe of the size of the initial soluble aggregates smaller than 0.45 μm; and finally, both a protein carbonylation assay and mass spectrometry were used to detect potential oxidation of the mAb after exposure to steel.

MATERIALS AND METHODS

Materials

The model monoclonal antibody (mAb) used in these studies was a humanized immunoglobulin-G_1 (IgG_1) antistreptavidin donated by Amgen Inc. (Thousand Oaks, CA). This mAb is not a commercial or development product. The IgG_1 mAb has the properties: molecular weight, M = 145 kDa (including 3 kDa glycosylation); UV absorption coefficient at 280 nm, $A_{1\%}$ = 15.86; isoelectric point, pI = 8.7; and hydrodynamic diameter, D_h = 10.5 ± 0.5 nm. This mAb solution contained ~ 2% dimer as received. In this study we formulated the mAb in 10 mM sodium acetate at pH 5.0 ("buffer").

Stainless Steel Microparticles

The stainless steel microparticles were the same as used in our previous study and donated by Ametek, Inc. (Eighty Four, PA).[6] Properties of the stainless steel: BET specific surface area, 0.15 ± 0.01 m^2/g; particle size, 14 ± 1 μm; ζ-potential in buffer, −11 ± 1 mV.[6] The steel particles have a relatively smooth irregular globular morphology and passed the test for passivation.[6]

Protein and Soluble Aggregate Assays

Size exclusion chromatography (SEC) was used to quantify mAb monomer and soluble aggregate levels. SEC was performed with a TSK-GEL $G3000SW_{XL}$ column and SW guard column (Tosoh Bioscience LLC, Montgomeryville, PA). The mobile phase used consisted of 100 mM NaP_i, 300 mM sodium chloride, and 0.01% w/v sodium azide (pH 7.0) with a flow rate of 0.6 mL/min and UV detection at 280 nm.

Initial Rate Aggregation Kinetics Studies

Using initial rate kinetics studies we investigated whether the rate of aggregation (r) of the mAb by exposure to stainless steel can be expressed with a simple kinetic expression such as: $r = k_A A_{steel}^m C_{mAb}^n$. To determine the reaction order (m) with respect to the stainless steel area per-unit-volume (A_{steel}, units of cm^2/mL) we prepared several sets of samples containing from 200 to 800 mg of stainless steel (about 300 to 1200 cm^2/mL) with 1.0 mL of 1.0 mg/mL mAb solution. This was enough steel area to adsorb up to about 12% of the mAb initially present. The samples were mixed in separate 1.7 mL polypropylene tubes for 30–60 min by end-over-end rotation at 8 rpm to allow the adsorption to occur and then 0.8 mL of each dispersion was transferred to individual 0.6 polypropylene microcentrifuge tubes so that the air-water interface was eliminated. Control samples were prepared without steel microparticles and analyzed in the same way. We corrected the stainless steel surface area per-unit-volume for the volume of the particles to obtain the actual area per-unit-volume in cm^2/mL of solution (about a 10% correction or less). To find the order of the reaction (n) with respect to mAb concentration (C_{mAb}, units of mg/mL) we prepared individual vials with 300 mg of stainless steel particles and added 1.0 mL of mAb at 1.0, 2.2, 8.9, and 10.7mg/mL (the steel surface area was 425 cm^2/mL). The Carnahan–Starling hard-sphere model equation was used to make the small correction to convert mAb concentrations to activities by accounting for excluded volume non-idealities.[13] The samples were diluted as appropriate to obtain a concentration of around 1 mg/mL and then analyzed by SEC. Linear regressions were used to fit the initial aggregation rate data. The increase in aggregates level (measured aggregates minus the initial aggregates level) was used in the analysis so that any aggregates co-eluting with the dimer peak (present at ca. 2% in the stock solution) would be included in the increase in aggregates measure.

Effect of Polysorbate Surfactant on the Aggregation Rate

We performed an additional incubation study with protein at 1 mg/mL formulated with 0.1% w/v polysorbate 20 (PS20) to evaluate whether the surfactant could suppress aggregation of the mAb induced by 425 cm^2/mL stainless steel.

Determination of Reversibility of mAb Adsorption to Stainless Steel using Fluorescence Labeling

In our previous work we found that the adsorption of the mAb to stainless steel was irreversible with respect to dilution in buffer and also irreversibly adsorbed after resuspension of the mAb-adsorbed-to-steel in phosphate-buffered saline (PBS). This contrasted with the fact that about 63% of mAb could be desorbed from glass after resuspension in PBS.[6] These prior studies of the reversibility of adsorption did not address whether exchange between the adsorbed and the solution mAb could occur. We used fluorescent labeling of the mAb to detect whether the mAb would desorb from stainless steel under various conditions.

We used AlexaFluor® 488 protein labeling kit (Molecular Probes Inc., Eugene, OR) to label the mAb using amine-reactive chemistry according to the supplied protocol. We used five times the recommended protein concentration and found that each mAb was labeled with an average of 1.2 dye molecules. This material was diluted into unlabeled mAb to 12.5% of 1.0 mg/mL.

The reversibility study was performed by adsorbing 37.5 μg of the diluted labeled mAb stock solution to 500 mg of stainless steel (representing a surface area of 750 cm^2) in 2 mL total volume: about twice the steel needed to adsorb all of the mAb from solution. A control was prepared without any added steel and the fluorescence intensity of the labeled mAb determined with excitation at 494 nm and emission over the range 500 to 600 nm (peak at 519 nm). The fluorescence was measured on an SLM Aminco fluorometer (SLMAminco, Urbana, IL).

Dynamic Light Scattering of Aggregates

Samples for protein aggregate size determination were prepared by addition of 1.8 mL of mAb at 2.3 mg/mL to 540 mg of stainless steel (about 450 cm^2/mL of steel area) so that 1.7 mL polypropylene microcentrifuge tubes would be overfilled to minimize the air-water interface to a residual bubble up to 4 mm in diameter. Controls were prepared without stainless steel. Triplicate samples were incubated at 23°C and 8 rpm end-over-end rotation for up to about 4 days. Dynamic light scattering was performed on the samples after allowing the steel to settle under gravity and then filtering the supernatant through a 0.45 μm syringe filter to remove any residual large steel particles. The very low light scattering counts, similar to a filtered buffer blank, for controls without protein showed that this method for removal of steel particles was effective. Data were collected on a Brookhaven Light Scattering System (Brookhaven Instrument Corporation, Holtsville, NY) for 1 min using a 633 nm laser. Data were analyzed using the CONTIN method to determine the size distribution.

Mass Spectroscopic Analysis of mAb Aggregates formed by Exposure to Stainless Steel

We used mass spectrometry to profile the tryptic digest fragments of the mAb after exposure to stainless steel. We used this method to look for signs of methionine oxidation, which has been known to result in protein aggregation. Methionine is one of the amino acids most susceptible to oxidation.[10,14–20] A stressed sample was prepared by addition of 4 g (representing a surface area of ca. 6000 cm^2) of stainless steel to about 15 mL of mAb at 0.2 mg/mL in an overfilled polypropylene tube that was mixed by end-over-end rotation at 8

rpm for 9 days. This sample contained about 70% soluble aggregates, according to SEC analysis. The sample was concentrated by centrifugal filtration to about 1 mg/mL before the unfolding/digestion preparation procedure for the mass spectrometry analysis. A reference control sample at 2.3 mg/mL without any stress was also measured. Additionally, the mAb adsorbed to the steel particles was treated in the same way as the supernatant to attempt to digest and obtain peptide fragments that had originally been part of the first layer of irreversibly adsorbed mAb.

The samples were incubated in 6 M guandine with 5 mM DTT for 2 hours at 37°C to cause unfolding of the mAb. They were then diluted from 0.5 to 4 mL in 25 mM TRIS buffer. Trypsin was added to 0.5 mL of the unfolded mAB at about $1/20^{th}$ ratio based on mass and incubated for 5 hours at 37°C. The proteolysis was quenched by freezing the samples at −80°C.

The samples were prepared for spotting on the Matrix Assisted Laser Desorption (MALDI) plate using ZipTip® (Millipore, Billerica, MA) C18 solid phase extraction to collect the peptide fragments. The samples were eluted and mixed into the α-cyano-4-hydroxycinnamic acid (CHCA) matrix and spotted on the MALDI sample plate. A set of standard peptides was also spotted as a calibration (ProteoMass® kit, ThermoFisher Scientific, Waltham, MA).

An Omniflex® (Bruker Daltonics, Bremen, Germany) instrument set for positive reflection mode was used to collect the mass spectra. Analysis was performed using the flexanalysis® and Biotools® software from Bruker.

Protein Carbonylation Test for mAb Oxidation

Protein carbonylation is the most general and abundant modification caused by many different mechanisms of protein oxidation.[21] We used the OxiSelect™ Protein Carbonyl Assay (Cell Biolabs Inc., San Diego, CA) to derivatize the carbonyls with dinitrophenylhydrazine (DNPH) which were then assayed by UV absorbance at 375 nm to determine the oxidation levels of the protein before and after steel exposure. Highly stressed samples were prepared as described for the mass spectrometry samples except they were measured after 29 days. The sample was concentrated by centrifugal filtration to about 2 mg/mL for the oxidation assay.

RESULTS AND DISCUSSION

Initial Rate Aggregation Kinetics Studies

Figure 1 shows the aggregates detected by SEC after incubation of 1 mg/mL mAb with 425 cm^2/mL of stainless steel area for 3 days. Triplicate samples at each time point were used to determine the initial aggregation rate. Figure 2 shows the initial aggregation rate data presented as a $\log_{10}$-$\log_{10}$ plot to determine the reaction order with respect to the steel surface area. The total aggregation was less than 5% of the mAb initially present. Because the study was conducted at this low fractional conversion of monomer to aggregates, determination of the aggregation rate parameters by quantification of the appearance of aggregates resulted in data with less variability than following the decrease in the monomer-associated SEC peak. In this work the monomer loss and aggregates generation were consistent with exclusive generation of soluble aggregates within the assay quantification limits and variability. It is possible that colloidal instability in the primary soluble aggregates could lead to a secondary condensation into larger insoluble aggregates after prolonged periods of time. Overall, we found that the aggregation process was second-order in steel surface area. A regression fit to the aggregates generation data gave a reaction order

(slope) of 2.1 ± 0.3 (r^2 = 0.88). Fixing the slope at 2.0 ± 0.3 gives an equally good fit (r^2 = 0.88) with an intercept of −4.6 ± 0.9 (quoted errors are standard errors of the fits).

Figure 3 shows a $\log_{10}$-$\log_{10}$ plot of the concentration studies data showing that the data is consistent with a zero-order dependence in protein concentration. The solid line is a prediction based upon a zero-order reaction rate. The aggregation rates for the 1 and 10.7 mg/mL samples were measured for up to 3 days. We found that only 10 μg/mL of aggregates was formed after 2 days: this represents 1% aggregation of the 1 mg/mL sample and only 0.1% aggregation of the 10 mg/mL sample. For this reason, we were better able to follow the increase in soluble aggregates because there was less error in the integration of the new peak formed than the small decrease in monomer peak. The samples at 2.3 and 8.9 mg/mL mAb were measured at various times from 5 to 17 days in order to evaluate whether the rate changed over longer times. These samples had a slightly lower aggregation rate than the samples measured for the first few days that is not explained by a simple concentration dependence of the rate since the conversion to aggregates was so low and the order is zero with respect to concentration. We suggest that a decrease in the reactivity of the steel surface with time, possibly due to fouling of the surface with protein aggregates, could explain this result. This would be analogous to the well-known phenomenon of catalyst poisoning by irreversible adsorption of a product or side-product.[11] For this subtle aggregation, SEC with UV detection is not suitable for detecting aggregation for more concentrated samples: preliminary studies with samples at 56, 93 and 142 mg/mL mAb did not result in any quantifiable aggregation (within the limits of the assay and dilution variability) within a week. This fact is also consistent with a zero-order dependence on the mAb concentration. These results also indicate that there is no concentration-dependent nucleation of aggregation by another mechanism occurring over the practical mAb formulation ranges.

The initial rate kinetic data are consistent with a rate-determining aggregation step that is second-order in steel surface area (cm^2/mL) and zero-order in mAb concentration over the range 1 to 10 mg/mL and 300 to 1200 cm^2/mL of steel area, specifically: $r = k_A A_{steel}^2$. From the intercept of the steel rate study we calculate that the rate constant, k_A, is 0.03 $ng \cdot mL \cdot day^{-1} \cdot cm^{-4}$

A Simple Mechanism Consistent with the Measured Reaction Orders

The aggregation we observe is second-order in surface area and zero-order in concentration, consistent with a mechanism that is dominated by surface adsorption.[11] With reference to classic Langmuir-Hinshelwood kinetics a bi-molecular surface reaction rate-limiting step could give the experimental data we observed.[11] The following derivation shows one simple reaction scheme (but not unique) that would result in the observed rate dependencies. To find the predicted reaction orders, we limited the complexity of the mathematics by assuming dimer aggregates would desorb from the surface. Symbols and subscripts represent: native protein monomer, *P*; free surface site, *S*; dimer aggregate, D_2; total surface area, T; adsorbed protein, *P·S*. The mAb concentrations is represented as "*C*" (units of mg/mL), the surface area concentrations as "*A*" (units of cm^2/mL), equilibrium constants as "*K*", and the rate-limiting step rate constant as k_A

$$\text{Adsorption: } P + S \rightleftharpoons P \cdot S; \text{ where } K_{P \cdot S} = A_{P \cdot S} / C_P A_S$$

$$\text{Surface aggregation: } P \cdot S + P \cdot S \xrightarrow{k_A} D_2 + 2S; \text{ and } r = k_A A_{P \cdot S}^2$$

$$\text{Surface area balance: } A_T = A_S + A_{P \cdot S}$$

$$\text{rate equation: } r = k_A A_{P \cdot S}^2 = \frac{k_A A_T^2 (K_{P \cdot S} C_P)^2}{(1 + K_{P \cdot S} C_P)^2} : r = k_A C_T^2 \text{ when } K_{P \cdot S} C_P \gg 1$$

Since we observe formation of soluble aggregates larger than a dimer this simple derivation is far from a complete description of the actual aggregation. However, it does serve to demonstrate how the order dependence of the aggregation could arise. In the actual reaction, the limiting aggregate size in the bulk solution could be due to propagation of the aggregation on the surface until the aggregates detach at a certain size, or due to fast growth of the aggregates nucleated by steel to a limiting 'bottleneck' size of aggregates in the bulk. The rate-determining step would still be the bimolecular surface reaction and so still give the second-order in surface area dependence for these more complex reaction schemes. Other faster microscopic aggregation steps critical to the overall aggregation process (e.g. possibly oxidation) could be occurring with the rate still limited by the bimolecular surface reaction. The time evolution of the size, shape and location of the aggregates as the reaction proceeds could give more fundamental mechanistic insight but is beyond the scope of this foundation study. Specifically, it would be interesting in future studies to investigate whether the aggregate shapes are globular, chains, or fractal in nature and whether they grow upwards from the surface or outwards along the surface.

Effect of Polysorbate Surfactant on the Aggregation Rate

We found that PS20 at 0.1 % w/v effectively suppressed the aggregation of the mAb by stainless steel (Figure 4). There is an apparent inconsistency between the ability of PS20 to suppress aggregation that contrasts with its inability to cause mAb desorption from the first layer. This quandary is resolved if the 'reactive surface' is not the bare steel but actually the first layer of strongly bound mAb molecules, and the PS20 acts by competing with the mAb for adsorption onto subsequent multiple layers. It is also possible that PS20 binds with aggregate pre-nuclei to directly inhibit aggregate nucleation.

Reversibility of mAb Adsorption to Stainless Steel

An exchange study was performed by removing the excess buffer supernatant (verified to contain no labeled protein) from the steel with adsorbed labeled mAb and then adding 2 mL of unlabeled mAb at 1 mg/mL. No desorbed/exchanged mAb was detected in the supernatant after 16 hours of incubation. Subsequently, addition of up to 2% w/v polysorbate 20 with 5 min of mixing did not result in any desorption. Finally, addition of guanidine salt at 8 M did not result in any measurable labeled mAb desorption into the supernatant. Therefore even these quite aggressive solution conditions did not result in any detectable mAb desorption from the stainless steel.

As a positive control we repeated a similar study with mAb adsorbed to ground glass vials using similar calculations to determine the amount of glass needed (using results and materials from our previous published study[6]). We found that exchange did not occur between the labeled mAb adsorbed to glass and 1 mg/mL mAb in the supernatant. We also found that 2 % w/v polysorbate was unable to cause mAb desorption. However, we were able to recover 68% of the adsorbed labeled mAb by addition of 8 M guanidine salt to the solution. This is consistent with our previous work that showed 63% of mAb could be desorbed from glass in PBS.[6] Interestingly, it seems that the remaining adsorbed mAb on glass is also very irreversibly bound.

The labeling study showed that there is a very firmly bound monolayer of mAb adsorbed to the stainless steel surface whose adsorption is essentially irreversible. None of the mAb from this first adsorbed layer is released back into the bulk due to exchange or during the aggregation process. This result, along with fact that the aggregation is characterized almost exclusively by formation of soluble aggregates, leads to the logical conclusion that the actual 'reactive surface' with respect aggregation of the bulk mAb is not the bare steel surface but the first layer of adsorbed mAb. This first layer of steel-adsorbed mAb must be

perturbed by in such a way that it can effectively 'template' the aggregation of the bulk mAb. From the rate studies we know that the final aggregates are soluble, but reasonably large at about 200 nm (see DLS data in Figure 5). Together, these data are consistent with adsorption of mAb to form a second (or more) layers with strong self-interactions promoted by structural changes templated by the first adsorbed layer. One possibility is that larger aggregates could then be released if they have a lower affinity for adsorption after reaching a certain size.

One interesting point is that in our previous works we found that both cellulose and glass could preferentially adsorb aggregates, but only within certain formulation 'windows'.[6,22] This hints that there are very complex energetic balances occurring upon adsorption that can lead to all of these behaviors. The outcomes we have observed in our prior work are:[6,22] simple (near native) monolayer adsorption of mAbs; a first mAb layer that irreversibly binds aggregates; and a first mAb layer that binds additional layers resulting in appearance of soluble aggregates in the bulk. Other additional possibilities not observed in our studies, but observed in others' research,[8] are that the multilayer formation continues until larger nucleated particles are formed or until the smaller protein-coated particles coagulate. As a whole, this leads us to speculate that all of these different outcomes could possibly be a general phenomenon and potentially be observed for different surface/protein/formulation conditions. This means that changing formulation conditions could be a powerful tool to reduce any adverse protein-surface interactions by tipping the balance of interactions in a different direction. However, it also suggests that unexpected aggregation by surfaces could occur and this should be monitored.

Size of Soluble Aggregates

The cumulative size distributions from the DLS analysis of mAb incubated with steel for up to 4 days is shown in Figure 5. We found that within 30 min the aggregate peak at about 200 nm diameter was observed and that this same size aggregate was seen in all the samples up to 4 days of incubation. This result is consistent with a 'bottleneck' in the aggregation process that results in a maximum sized aggregate which then does not grow appreciably.[12] The surface-driven nature of this aggregation process leads us to the hypothesis that there may be multilayer formation and propagation of aggregates until they become too large to remain adsorbed to the surface. Another possibility is that an initial nucleus detaches from the surface and grows in the bulk until it also reaches a certain size limit. These results highlight very clearly that in this case the soluble aggregate at about 200 nm seems to be a natural limit of this aggregation process. We confirmed that re-reading samples from which the steel had been filtered out resulted in the same size distribution (i.e. no further growth of the 200 nm aggregates) for several days.

Mass Spectroscopic Analysis of mAb Aggregates formed by Exposure to Stainless Steel

We performed mass spectrometry to look for methionine (Met) residue oxidation since it has been implicated in protein aggregation.[10,14–19] No peaks that could be assigned to oxidation of either of the two Metresidues in the heavy chain (HC) were found in either the control or stressed samples (stressed samples contained about 70% soluble aggregates). All samples showed some signs of deamidation and Cys oxidation but also contained fragments for reduced Cys. The sequence coverages of the control and stressed samples were similar. The digest retrieved from the mAb adsorbed to the solid steel surface only gave peaks smaller than about 2400 Da, and the fragments containing the two Mets were not detected.

Overall, these mass spectrometry data provide no conclusive evidence to support the hypothesis that oxidation of Met is responsible for the observed aggregation of this mAb by exposure to stainless steel.

Protein Carbonylation Test for mAb Oxidation

Since protein oxidation could be mediated by Fe ions after structural perturbation due to adsorption, or potentially by a corrosive interaction of the mAb with the steel surface, we measured the oxidation levels in the aggregated mAb using a protein carbonyl assay. Protein carbonlyation is a stable product of protein oxidation caused by many oxidative stress mechanisms and is the most abundant modification caused by oxidation.[21] A typical baseline oxidation level is 0.05 mol of carbonyl per mol of protein which can increase by 2–8 times after in-vivo oxidative stress.[23] The oxidation levels for a control sample and for a highly aggregated sample exposed to steel for 29 days were 0.2 ± 0.1 and 0.8 ± 0.2 mol of carbonyl per mol of mAb respectively. This result shows there was about a four-fold increase in the carbonyl level in the highly stressed sample. Although the increase in carbonyl is correlated with aggregate formation, we note that oxidation and aggregation are not necessarily linked in terms of a cause-and-effect relationship. Fe ions leached from steel are a likely cause of this oxidation, yet they did not cause detectable Met oxidation.

Prediction of Storage Stability for this mAb Exposed to Steel

We calculate that storage of this mAb in a pre-filled syringe for 2 years with about 0.2 cm^2/mL of steel needle area would result in 1 ng/mL of aggregates by this steel-induced aggregation mechanism. This is an essentially undetectable level of aggregation. A small in-process container might have at most 1 cm^2/mL of steel area in contact the protein, generating aggregates at a rate of 0.03 $ng \cdot mL^{-1} day^{-1}$, also a minute level. We note that a seemingly insignificant mass of protein aggregates could still form a large number of sub-visible particles, which then could potentially coagulate or agglomerate to form larger, visible particles. For example, Tyagi et al. found that pumping a mAb solution through a reciprocating-piston fill-finish pump resulted in the generation of 300,000 sub-visible proteinaceous particles/mL but the mass loss was not significant within the error of the assay. In the same study, pumping of protein-free solutions only generated 13,000 detectable particles/mL but subsequent mixing of this pumped buffer with an un-pumped protein solution generated more, and larger particles.[8] The conclusions of these experiments were that particles of sizes below 1 μm (the detection limit of the particle counter) were shed from the pump and then interacted with the protein to generate much larger proteinaceous particles, even though the actual mass loss was undetectable.[8]

As a caveat, we note that other proteins may be much more sensitive to stainless steel, so these results are not generally predictive for other proteins or formulations. Also, we did not study any potential synergies of stainless steel exposure with other stresses such as shear (possibly increasing adsorption/desorption rates) or freeze/thaw cycles. Steel could also cause aggregation of this, or other proteins, with a higher rate constant in different formulations. We did not study long-term exposure effects in this work: other secondary processes like loss of the reactivity of the steel surface or aggregation by a slower leachate-based mechanism could possibly occur over much longer time scales than we studied here.

CONCLUSIONS

Stainless steel was found to induce aggregation of a mAb with a second-order dependence on the steel surface area and a zero-order dependence on the mAb concentration. Exposure to stainless steel surfaces also resulted in an increase in carbonylated degradation products. Extrapolation of the aggregation rate for 2 years of storage in a pre-filled syringe predicts only minute levels of protein mass lost to aggregation. Although the rates of these surface-mediated reactions to produce sub-visible aggregates are relatively slow, we speculate that, in some cases, upon storage these sub-visible particulates could assemble to visible aggregates that could compromise product quality.

Acknowledgments

Funding for this work was provided by the Graduate Assistantship in Areas of National Need (GAANN) program, the NIH Leadership in Pharmaceutical Biotechnology program (NIH T32 GM008732), the NIH (NIH NIBIB Grant 1 R01 EB006006-01), and Amgen Inc. We thank Christopher Roberts for useful discussions.

Abbreviations

mAb	monoclonal antibody
SEC	size exclusion chromatography
UV	ultraviolet

REFERENCES

1. Schellekens H. Immunogenicity of therapeutic proteins: Clinical implications and future prospects. Clinical Therapeutics. 2002; 24(11):1720–1740. [PubMed: 12501870]
2. Rosenberg AS. Effects of protein aggregates: An immunologic perspective. Aaps Journal. 2006; 8(3):E501–E507. [PubMed: 17025268]
3. Randolph TW, Carpenter JF. Engineering challenges of protein formulations. AIChE Journal. 2007; 53(8):1902–1907.
4. Chi EY, Krishnan S, Randolph TW, Carpenter JF. Physical Stability of Proteins in Aqueous Solution: Mechanism and Driving Forces in Nonnative Protein Aggregation. Pharmaceutical Research. 2003; 20(9):1325–1336. [PubMed: 14567625]
5. Weiss WF, Young TM, Roberts CJ. Principles, Approaches, and Challenges for Predicting Protein Aggregation Rates and Shelf Life. Journal of Pharmaceutical Sciences. 2009; 98(4):1246–1277. [PubMed: 18683878]
6. Bee JS, Chiu D, Sawicki S, Stevenson JL, Chatterjee K, Freund E, Carpenter JF, Randolph TW. Monoclonal Antibody Interactions with Micro- and Nanoparticles: Adsorption, Aggregation and Accelerated Stress Studies. Journal of Pharmaceutical Sciences. 2009
7. Biddlecombe JG, Craig AV, Zhang H, Uddin S, Mulot S, Fish BC, Bracewell DG. Determining antibody stability: Creation of solid-liquid interfacial effects within a high shear environment. Biotechnology Progress. 2007; 23(5):1218–1222. [PubMed: 17715937]
8. Tyagi AK, Randolph TW, Dong A, Maloney KM, Hitscherich C, Carpenter JF. IgG particle formation during filling pump operation: A case study of heterogeneous nucleation on stainless steel nanoparticles. Journal of Pharmaceutical Sciences. 2009; 98(1):94–104. [PubMed: 18454482]
9. Wang W, Singh S, Zeng DL, King K, Nema S. Antibody structure, instability, and formulation. Journal of Pharmaceutical Sciences. 2007; 96(1):1–26. [PubMed: 16998873]
10. Lam XM, Yang JY, Cleland JL. Antioxidants for prevention of methionine oxidation in recombinant monoclonal antibody HER2. Journal of Pharmaceutical Sciences. 1997; 86(11):1250–1255. [PubMed: 9383735]
11. Fogler, HS. Elements of Chemical Reaction Engineering. 4 ed.. Upper Saddle River, NJ: Pearson Education Inc.; 2006.
12. Roberts CJ. Non-native protein aggregation kinetics. Biotechnology and Bioengineering. 2007; 98(5):927–938. [PubMed: 17705294]
13. Alford JR, Kendrick BS, Carpenter JF, Randolph TW. High concentration formulations of recombinant human interleukin-1 receptor antagonist: II. aggregation kinetics. Journal of Pharmaceutical Sciences. 2008; 97(8):3005–3021. [PubMed: 17924426]
14. Reubsaet JLE, Beijnen JH, Bult A, Hop E, Scholten SD, Teeuwsen J, Underberg WJM. Oxidation of recombinant methionyl human granulocyte colony stimulating factor. Journal of Pharmaceutical and Biomedical Analysis. 1998; 17(2):283–289. [PubMed: 9638581]
15. Liu HC, Gaza-Bulseco G, Xiang T, Chumsae C. Structural effect of deglycosylation and methionine oxidation on a recombinant monoclonal antibody. Molecular Immunology. 2008; 45(3):701–708. [PubMed: 17719636]

16. Duenas ET, Keck R, De Vos A, Jones AJS, Cleland JL. Comparison between light induced and chemically induced oxidation of rhVEGF. Pharmaceutical Research. 2001; 18(10):1455–1460. [PubMed: 11697472]

17. Griffiths SW, Cooney CL. Relationship between protein structure and methionine oxidation in recombinant human alpha 1-antitrypsin. Biochemistry. 2002; 41(20):6245–6252. [PubMed: 12009885]

18. Soenderkaer S, Carpenter JF, van de Weert M, Hansen LL, Flink J, Frokjaer S. Effects of sucrose on rFVIIa aggregation and methionine oxidation. European Journal of Pharmaceutical Sciences. 2004; 21(5):597–606. [PubMed: 15066660]

19. Liu JL, Lu KV, Eris T, Katta V, Westcott KR, Narhi LO, Lu HS. In vitro methionine oxidation of recombinant human leptin. Pharmaceutical Research. 1998; 15(4):632–640. [PubMed: 9587962]

20. Thirumangalathu R, Krishnan S, Bondarenko P, Speed-Ricci M, Randolph TW, Carpenter JF, Brems DN. Oxidation of methionine residues in recombinant human interleukin-1 receptor antagonist: Implications of conformational stability on protein oxidation kinetics. Biochemistry. 2007; 46(21):6213–6224. [PubMed: 17480058]

21. Stadtman ER, Levine RL. Free radical-mediated oxidation of free amino acids and amino acid residues in proteins. Amino Acids. 2003; 25(3–4):207–218. [PubMed: 14661084]

22. Bee, JS.; Chiu, D.; Stevenson, JL.; Chatterjee, K.; Freund, E.; Carpenter, JF.; Randolph, TW. pH and Salt Effects on the Interactions of a Monoclonal Antibody with Glass. Manuscript-in-preparation for PhD thesis. 2009.

23. Shacter E. Quantification and significance of protein oxidation in biological samples. Drug Metabolism Reviews. 2000; 32(3–4):307–326. [PubMed: 11139131]

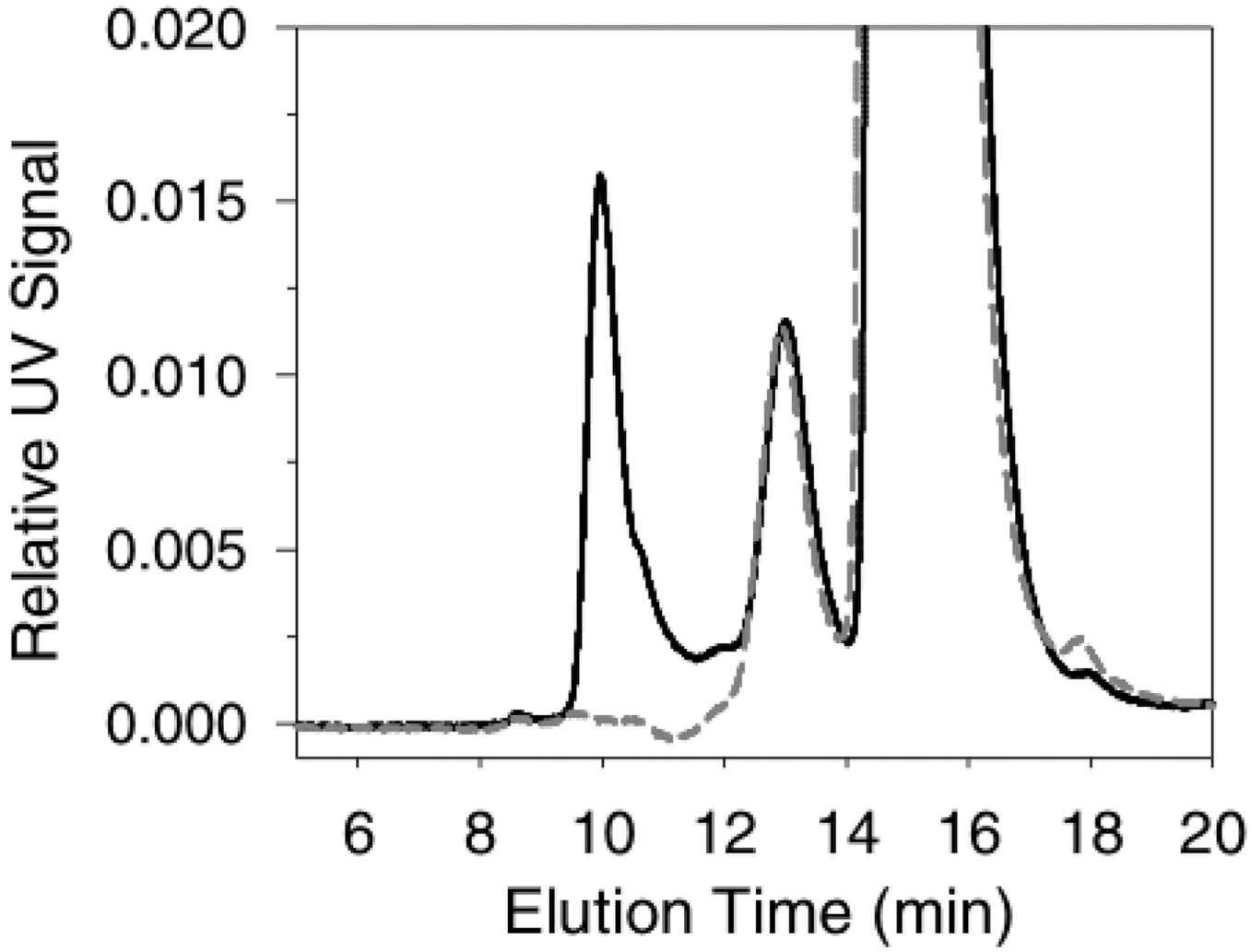

Figure 1.
Size exclusion chromatogram (SEC) of mAb after incubation with stainless steel. Data is representative of the aggregation after 3 days incubation of 1 mg/mL mAb with 425 cm^2/mL steel area. Control mAb, short-dashed gray line; after incubation with steel, solid black line. Peaks: monomer at 15.5 min; dimer/aggregates at 13 min; soluble aggregates at 10 min; fragment at 18 min.

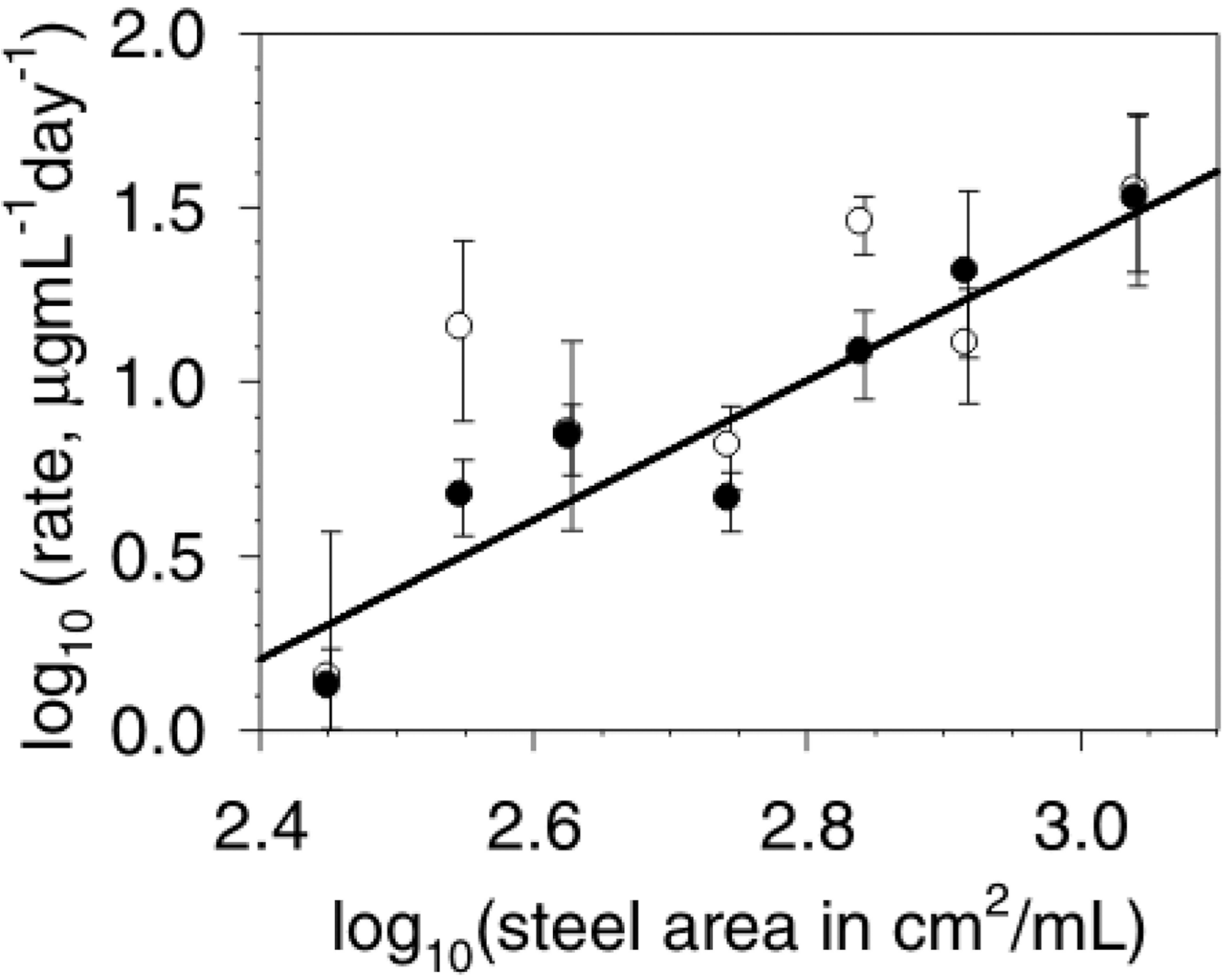

Figure 2.

Initial rate of aggregation as a function of steel surface area. The mAb was at 1.0 mg/mL. Data is presented as a $\log_{10}$-$\log_{10}$ plot. Data is the average aggregation rate and the error bars represent the 95% confidence interval of the aggregation rates. Rate data from: soluble aggregates appearance (●); decrease in monomer levels (○). The line represents the regression fit to the increase in soluble aggregates data with the slope fixed at 2.0 ± 0.3 (r^2 = 0.88), with intercept of −4.6 ± 0.9 (quoted errors are standard errors of the fit). Allowing the slope to float results in a slope of 2.1 ± 0.3 (r^2 = 0.88) and so is not significantly different than a slope of 2.0. The fit to the monomer loss data gives a slope of 1.7 ± 0.6, and intercept of −4 ± 2with r^2 = 0.6.

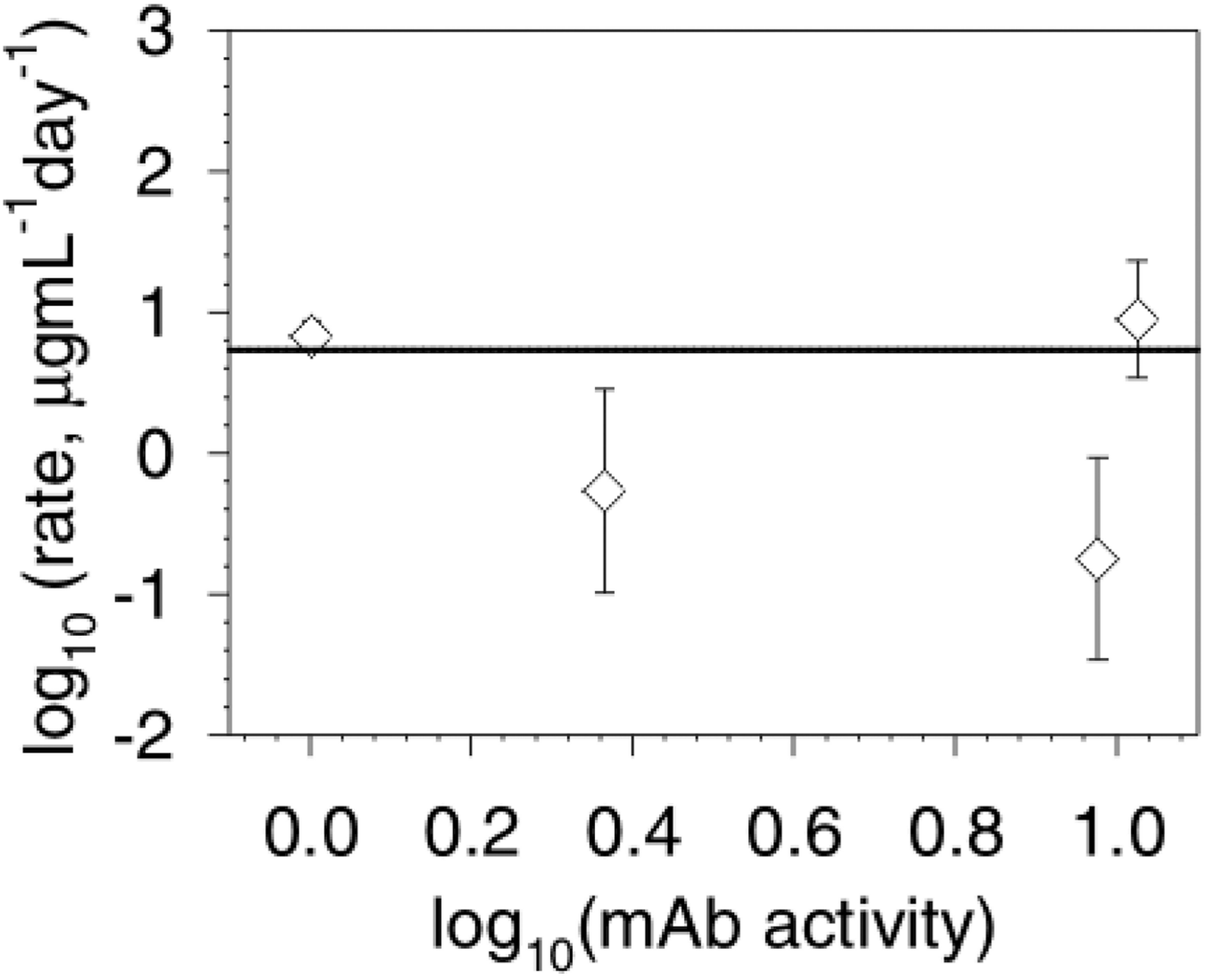

Figure 3.

Initial rate of aggregation as a function of mAb concentration. Data is presented as a $\log_{10}$-$\log_{10}$ plot. The concentrations in mg/mL were converted to thermodynamic activities. The steel surface area was 425 cm^2/mL. Data is the average aggregation rate and the error bars represent the 95% confidence interval of the aggregation rates. This data does not fit well to a trend-line (r^2 =0.06). The plotted line represents the prediction for a reaction that is second-order in steel area and zero-order in mAb thermodynamic activity. The data at 2.3 and 8.9 mg/mL were collected between 5 and 17 days to allow for (potentially) more conversion. The 1 and 10 mg/mL data points represent the aggregation over the initial 2–3 days.

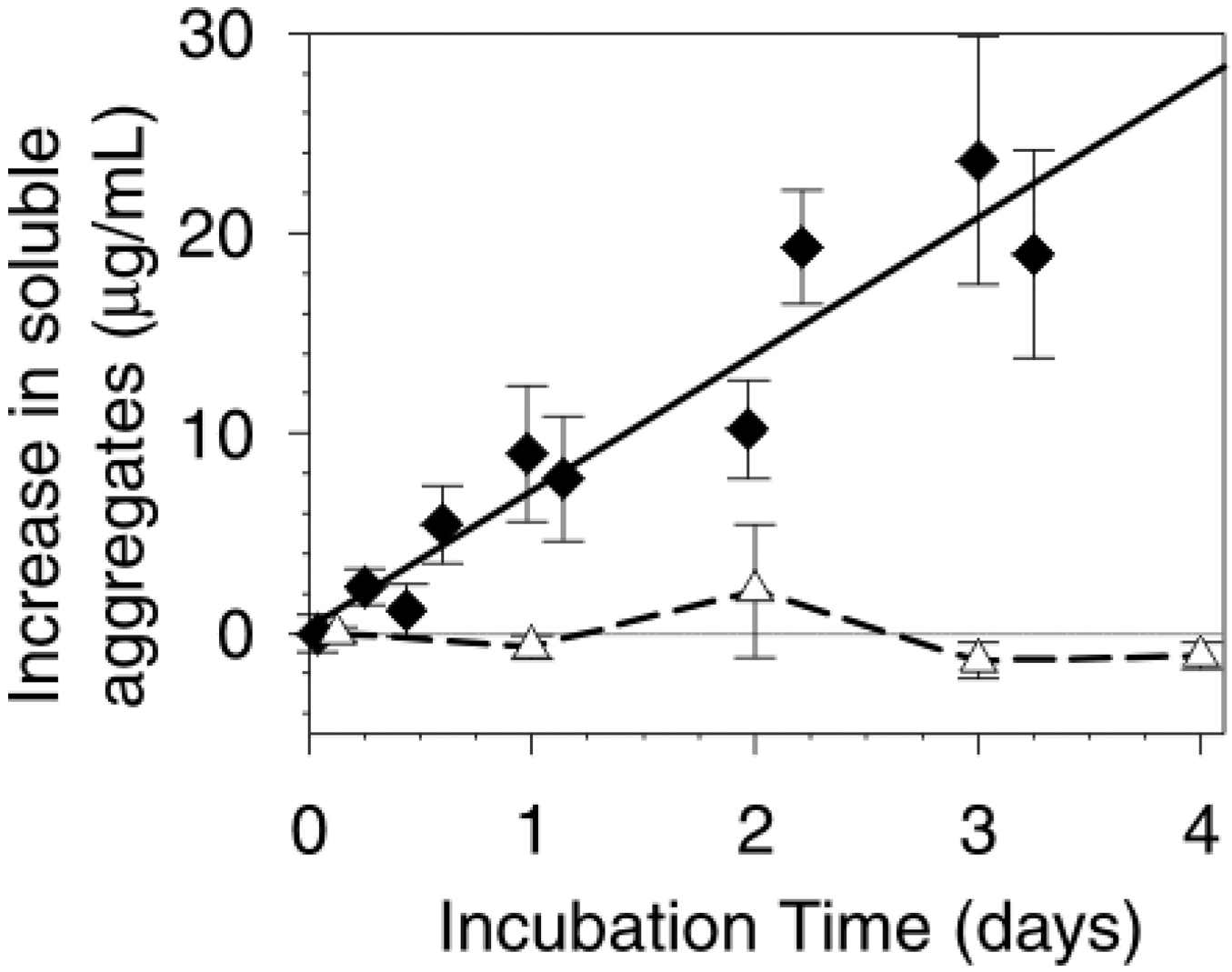

Figure 4.

Effect of 0.1 % w/v polysorbate 20 (PS20) on the rate of mAb aggregation. The mAb concentration was 1 mg/mL, with 425 cm^2/mL steel. Data are the average of the increase in aggregates level for each time point ±SD. The increase in aggregates level is defined as the measured aggregates minus the initial aggregates level. The data was analyzed this way so that any aggregates co-eluting with the dimer peak (present at ca. 2% in the stock solution) would be included in the increase in aggregates measure. Data: 1 mg/mL mAb, solid line (♦); 1 mg/mL mAb with 0.1 % w/v PS20 (Δ).

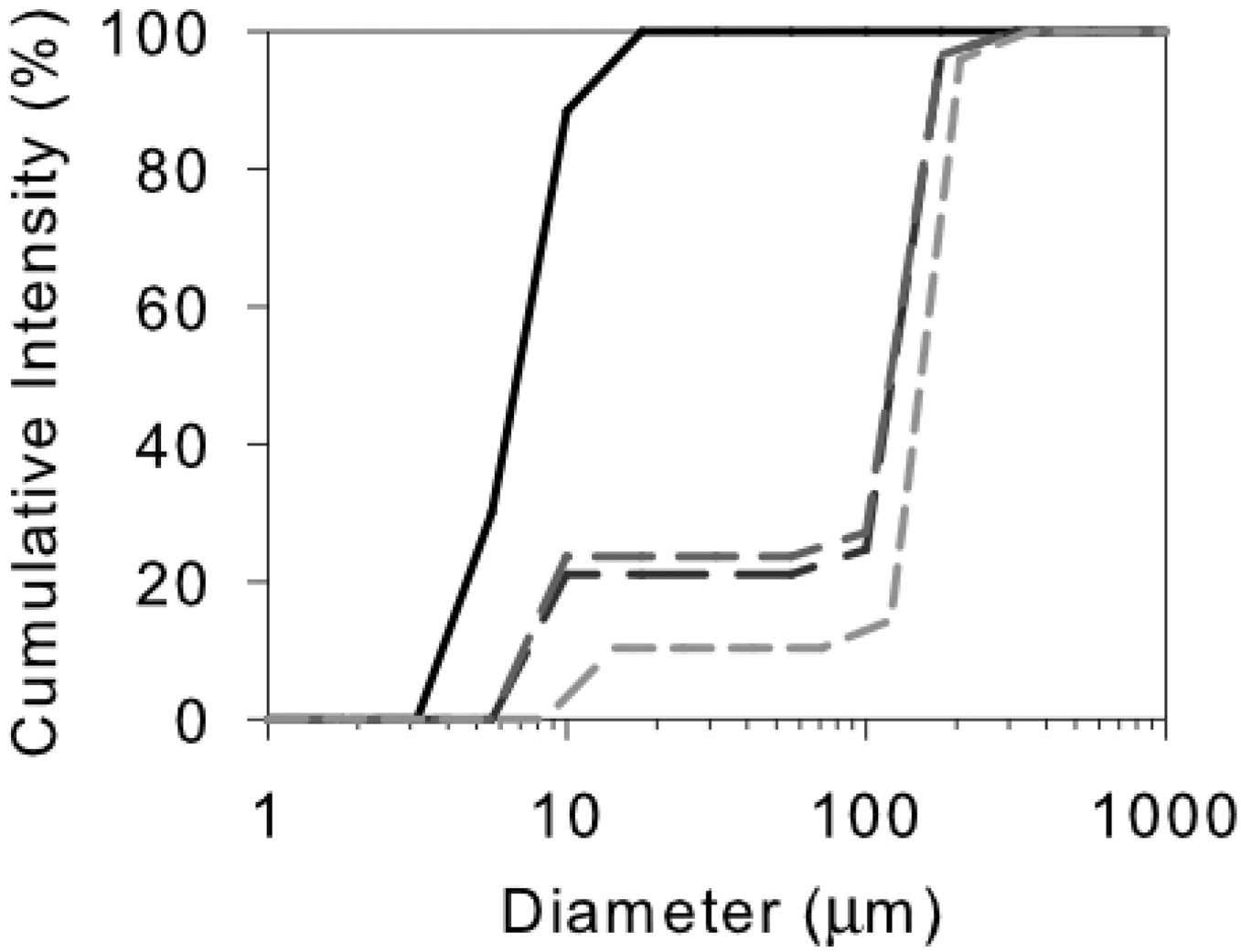

Figure 5.
Cumulative size distributions of mAb after exposure to steel. Cumulative intensities: control mAb, solid black line; after 30 min, long-dash line; after 20 hours; medium-dash line; after 4 days, short-dash light gray line. Each distribution is a single result representative of triplicate samples. The monomer is about 10 nm and the soluble aggregates about 200 nm in diameter.